

NASA TECHNICAL NOTE



NASA TN D-2137

c.1

LOAN COPY: F
AFWL (W
WESTLAND AE



TECH LIBRARY KAFB, NM

NASA TN D-2137

AN ANALYSIS OF ERRORS IN THE GEOGRAPHIC REFERENCING OF NIMBUS CLOUD PICTURES

by Eugene M. Darling, Jr.

*Goddard Space Flight Center
Greenbelt, Maryland*



**AN ANALYSIS OF ERRORS IN THE GEOGRAPHIC REFERENCING
OF NIMBUS CLOUD PICTURES**

By Eugene M. Darling, Jr.

**Goddard Space Flight Center
Greenbelt, Maryland**

NATIONAL AERONAUTICS AND SPACE ADMINISTRATION

**For sale by the Office of Technical Services, Department of Commerce,
Washington, D.C. 20230 -- Price \$0.75**

AN ANALYSIS OF ERRORS IN THE GEOGRAPHIC REFERENCING OF NIMBUS CLOUD PICTURES

by

Eugene M. Darling, Jr.

Goddard Space Flight Center

SUMMARY

Errors in the determination of satellite attitude from telemetered data are expected to cause a maximum overall error of 50 naut. mi. in the geographical referencing of Nimbus A cloud pictures. This error is tolerable for most operational purposes. For future Nimbus vehicles it is anticipated that this error can be reduced to less than 20 naut. mi.

CONTENTS

Summary	i
INTRODUCTION	1
DESCRIPTION OF THE NIMBUS ATTITUDE CONTROL SYSTEM	2
Pitch and Roll Attitude Control	2
Yaw Attitude Control	3
SOURCES OF ERROR IN THE ATTITUDE CONTROL SYSTEM	4
Input Signal	4
Control System	5
Momentum, White Noise and Telemetry Scale	5
ATTITUDE ERRORS FOR VARIOUS PROCEDURES	5
Disregard Telemetered Attitude Data	6
Use Telemetered Attitude Data	6
Scanner Pulse Reconstruction	6
THE EFFECT OF ATTITUDE ERRORS ON THE ACCURACY OF GEOGRAPHIC REFERENCING	7
Gridding Errors-Nimbus A	8
Gridding Errors-Future Nimbus Satellites	8
METEOROLOGICAL ASPECTS OF GRIDDING ERRORS	10
Winds and Clouds	10
Errors in Mean Cloud Properties	11
Accuracy Requirements for Cloud Location	12
SUMMARY AND CONCLUSIONS	13
References	13
Appendix A—Scanner Pulse Reconstruction	15
Appendix B—Mathematics of Gridding Errors	17

AN ANALYSIS OF ERRORS IN THE GEOGRAPHIC REFERENCING OF NIMBUS CLOUD PICTURES

(Manuscript received July 22, 1963)

by

Eugene M. Darling, Jr.
Goddard Space Flight Center

INTRODUCTION

Both operational and research applications of satellite cloud data require that geographic referencing be superimposed on the pictures. This referencing—or gridding as it is usually called—may take the form of either latitude and longitude lines or gridpoints defined by latitude-longitude intersections.

If the orientation of the satellite relative to the earth were known exactly then it would be possible to compute perfect grids by transforming focal plane coordinates into spherical coordinates on the earth, or vice versa. However, in reality the satellite attitude is never known exactly, hence the coordinate transformations operate on erroneous input data and therefore produce incorrect grids.

This paper analyzes the effect of attitude stabilization errors on the accuracy of geographic grids computed for Nimbus cloud pictures. Two introductory sections contain technical material pertinent to the problem. The first section provides the necessary background information on the operation of the control system; in the second section the sources of mechanical, optical, and electrical error in the system are discussed and the maximum magnitude of each contributing factor is estimated in terms of its effect on satellite attitude. Next the computations of attitude errors resulting from various techniques for manipulating telemetry data are presented. Up to this point, the discussion will have been concerned entirely with the problem of satellite orientation. However, in the following section the effect of attitude errors on geographic referencing is explored. Estimates of gridding errors for both Nimbus A and for future Nimbus satellites are presented.

In the final section the question of satellite data referencing is discussed in the broad context of location accuracy for related conventional meteorological data. Errors in the computation of mean cloud properties for grid squares are analyzed. An objective criterion is developed for determining the grid size compatible with a prescribed confidence level and a known gridding error.

DESCRIPTION OF THE NIMBUS ATTITUDE CONTROL SYSTEM

The portion of the Nimbus system which controls motions about the pitch and roll axes consists of three elements: *horizon scanners* which detect the earth and provide the required input to the *horizon attitude computer* which calculates pitch and roll errors* for input to the *control system*, consisting of flywheels and pneumatics, which generates the torques on the spacecraft required to correct these errors. The yaw attitude is detected by an integrating rate gyro which generates an error signal input to the yaw flywheel in the control system. See References 1 and 2 for a detailed discussion of the control system.

Pitch and Roll Attitude Control

Scanner and Electronics

The detection device consists of two infrared scanners (IR1 and IR2) mounted on the control package (Figure 1). One scanner looks forward in the direction of the positive roll axis; the other looks backward. The scanner beam is directed in a conical path by a rotating prism in such a way that the beam intercepts both the earth and outer space in each sweep. The detected energy is focused on a bolometer through an optical system sensitive to the 12.5 to 18μ band of the infrared spectrum. The bolometer output, being proportional to the incident energy, is essentially zero when the scanner sees outer space; increases rapidly at the leading edge of the earth; remains more or less constant while the beam sweeps across the earth; then drops sharply back to zero at the trailing edge of the earth.

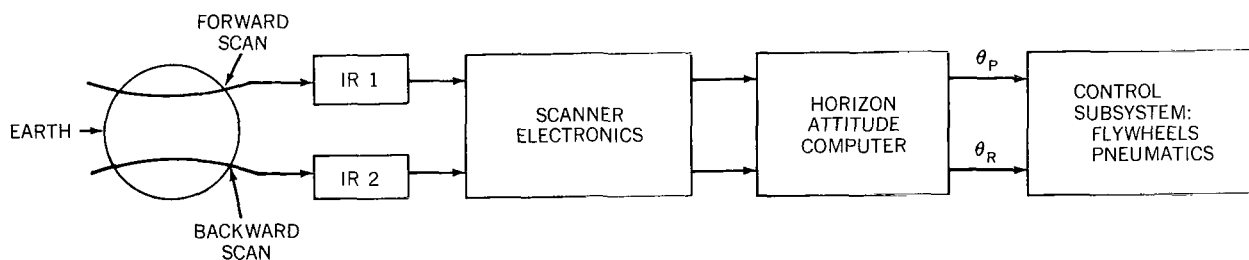


Figure 1—Pitch and roll attitude control, where θ_P is the pitch error signal and θ_R the roll error signal.

Electronic circuits in the scanner system filter the bolometer output to produce a smooth wave form for input to a pulse reconstructor in which a square pulse is constructed from the original wave. Whenever the reconstructor detects an energy of 480 mv at the leading edge of a wave it

*Any angular departure of a satellite body axis from its nominal orientation produces an attitude error. The nominal axis positions are:

Yaw: in the orbital plane perpendicular to the orbit. Positive towards the earth

Roll: in the orbital plane perpendicular to the yaw axis. Positive in the direction of motion of the satellite

Pitch: perpendicular to the orbital plane. Positive to the right of the satellite direction of motion

The components of attitude error are defined as follows:

Yaw: rotation about the yaw axis so that the roll axis no longer lies in the orbital plane

Roll: rotation about the roll axis so that the yaw axis no longer lies in the orbital plane

Pitch: rotation about the pitch axis so that the yaw axis is no longer perpendicular to the orbit

marks the beginning of a pulse. The end of the pulse is marked when the trailing edge of the wave reaches zero output. The square pulse fed to the horizon attitude computer begins and ends at the points determined by the above criteria.

Horizon Attitude Computer

The horizon attitude computer operates on the square pulses received from the scanner system. Pitch error is obtained by properly weighting the difference in width between the front and rear scanner pulses. Roll error is computed by weighting the difference in pulse length to the left and right of a magnetic reference which indicates the center of the pulse. Either the front or the rear pulse is used in this computation, depending upon the magnitude of the roll error. Pitch and roll errors are computed alternately and applied to a digital-to-analog converter which furnishes the proper error signal to the flywheels and pneumatics.

Control Subsystem

The pitch and roll attitude control loops both operate in the same manner. The error signal is fed to a flywheel amplifier which provides a control voltage to the momentum generator motor, thereby accelerating the flywheels by the amount required to produce the necessary restoring torque. If a specified threshold attitude error occurs then a signal is fed to a solenoid-controlled valve which permits gas to escape until the error falls below the threshold value. Also, in the event that either the pitch or roll flywheels reach 85 percent of maximum rated speed, pneumatic gating will occur (i.e. firing of a 0.52 second pulse of gas to dump flywheel momentum while at the same time providing the proper restoring torque).

Yaw Attitude Control

An integrating rate gyro (Figure 2) is mounted in the roll-yaw plane with its input axis inclined 12° with respect to the roll axis. This gyro senses yaw error as a component of the orbital pitch rate in the roll-yaw plane. The gyro electronics produces an error signal which is a linear function of yaw error, yaw rate, roll error and roll rate plus other small acceleration terms. The gyro output signal drives the yaw momentum motor which accelerates the flywheel by the proper amount. Pneumatic gating occurs at 65 percent of the maximum rated flywheel speed.

A yaw bias can be inserted by ground command in increments of 6° up to a maximum value of 30° . The purpose of this feature is to achieve maximum paddle insolation in the event that the satellite orbit departs from the sun-earth plane.

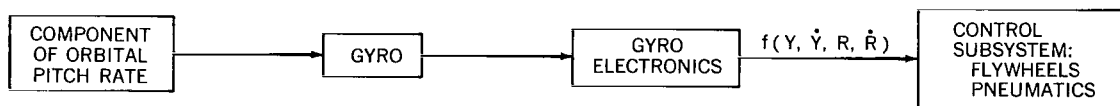
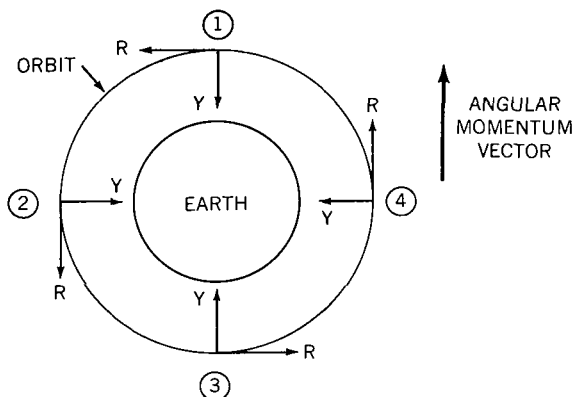


Figure 2—Yaw attitude control, where Y is the yaw error; \dot{Y} the yaw rate; R the roll error; and \dot{R} the roll rate.

Cyclic Momentum Exchange

In the absence of pneumatic gating, meteorite impact, gravitational gradients or other external torques the resultant momentum vector of the satellite and its three flywheels remains fixed in inertial space. This condition is maintained by a cyclic interchange of momentum between the roll



and yaw axes (Figure 3). The flywheel loops for roll and yaw are designed to take advantage of this momentum exchange in such a way that the removal of roll momentum by yaw substantially reduces the occurrence of roll gating. This design effectively minimizes the cross coupling between roll and yaw.

Figure 3 shows the normal cyclic variation in roll and yaw (in the absence of gating) resulting from flywheel operation. The error curves for roll and yaw each have an amplitude of about 0.8° ; the two curves are out of phase by 90° .

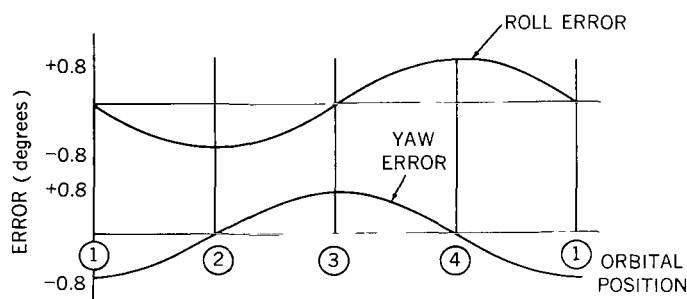


Figure 3—Cyclic momentum exchange between the roll R and yaw Y axes.

roll and yaw. However, the residual component along the pitch axis will result in a small, constant pitch error since the pitch momentum is not involved in the cyclic exchange mechanism. The maximum attitude error due to this effect is estimated to be about one half a degree.

Constant Pitch Error

At the end of the initial stabilization phase it is likely that the spacecraft will retain a certain residual momentum which will be transferred to the flywheels. This initial flywheel momentum will be incorporated in the cyclic exchange between

SOURCES OF ERROR IN THE ATTITUDE CONTROL SYSTEM

Each component of the control system contributes to the total error in satellite attitude. The pertinent error-producing factors may be conveniently grouped into five categories. The maximum attitude error contributed by each category is listed in Table 1a.

Input Signal

The effect of clouds on the earth's horizon is to place a cold radiating surface in the path of the scanner beam. As a result the energy level sensed by the bolometer is intermediate between that of space and a cloud-free earth. Based upon theoretical calculations which have been verified

by data from the Discoverer satellite the best estimate of the maximum energy ratio between a cloud-free and cloudy horizon is 2 to 1 (Reference 3). In calculating the pitch and roll errors shown in Table 1a this 2 to 1 ratio has been applied in the manner which produces the maximum error. Since yaw is under gyro control the above type of input signal error is not present.

Control System

This category includes the total error introduced by the scanner system (both optical and electronic) and the horizon attitude computer. Component errors averaging $.05^\circ$ have been root-mean-squared to obtain the tabulated values for each axis. In the case of both pitch and roll, the largest error (0.25° in each axis) is caused by mechanical alignment of the scanner system. The greatest individual contribution to yaw error (0.3°) is stability of the gyro drift.

Momentum, White Noise and Telemetry Scale

The errors tabulated for roll and yaw are a consequence of the momentum exchange mechanism previously described. It should be noted that the roll and yaw errors are out of phase by 90° so that the maximum error in one is always accompanied by zero error in the other (Reference 4).

The error listed under White Noise is that which would result from the presence of 100 mv RMS white noise in each control loop.

Attitude errors are telemetered in an 8-bit code (i. e. scale of 0 to 127). Thus there is a limit to the accuracy with which such errors can be read on the ground. This error is listed under Telemetry Scale.

ATTITUDE ERRORS FOR VARIOUS PROCEDURES

We shall now consider the errors which would result from several different procedures for determining satellite attitude. The total error for each method is computed by summing the values

Table 1
Sources of Attitude Error.

Error Source		a. Maximum Attitude Error (degrees)		
		Pitch	Roll	Yaw
1. Input Signal		± 0.58	± 1.75	—
2. Control System		± 0.35	± 0.35	± 0.35
3. Momentum		± 0.45	± 0.75	± 0.82
4. White Noise		± 0.1	± 0.1	± 0.3
5. Telemetry Scale		± 0.06	± 0.06	± 0.06
Mode	Error Computation	b. Total Attitude Error for Various Modes of Operation (degrees)		
		Pitch	Roll	Yaw
Disregard Telemetry	1+2+3+4	± 1.5	± 3.0	$\pm 2.0^*$
Use Telemetry	1+2+4+5	± 1.1	± 2.3	$\pm 2.0^*$
Scanner Pulse Reconstruction				
Assume 2° Yaw Error	2+4+5	± 0.5	± 0.5	$\pm 2.0^*$
Measure Yaw Error	2+4+5	± 0.5	± 0.5	± 0.7

*It should be noted that the maximum yaw error for the first three methods has been entered as $\pm 2.0^\circ$ rather than the appropriate sum of component errors (see footnote page 6).

in Table 1a in a prescribed manner (Reference 5). Results are presented in Table 1b. It should be emphasized that errors computed in this way are maximum values. *Errors of this magnitude would occur only in the unlikely event that all contributing factors reached their maximum errors simultaneously and all with the same algebraic sign.*

Disregard Telemetered Attitude Data

This is the null case where the satellite is assumed to remain in nominal attitude at all times. Accordingly, attitude errors are assumed to be zero throughout and all telemetry data on attitude is disregarded. The maximum error for this case is the sum of the first four items in Table 1a.*

Use Telemetered Attitude Data

This technique entails the use of telemetered attitude data without modification. The fine pitch and fine roll signals are interpreted as exact values of pitch and roll attitude, respectively. With this method the errors due to momentum are eliminated since the telemetered values are measured with respect to the cyclic momentum variations. However, the errors due to telemetry scale must be considered. The total maximum error in this case is the sum of items 1, 2, 4 and 5 in Table 1a. Note that the errors in pitch and roll are somewhat less than in the previous method.

Scanner Pulse Reconstruction

The salient feature of Table 1a is the large contribution of input signal error (Reference 6) to the total error in pitch and roll. For both axes this source accounts for *more than half* the total error. Thus, it is obvious that any expedient for substantially reducing this input error would result in a significant decrease in pitch and roll attitude error. A technique for reconstructing the earth input pulse from telemetered data on scanner output has been considered. The mathematics of this technique is presented in Appendix A. In applying the method (Reference 7), we must first reproduce the actual (i. e. cloudy) input wave. An ideal (i. e. no clouds) input wave of the same wavelength as the actual wave is then constructed and fed through an analog simulation of the scanner system. Both the ideal and actual scanner outputs are used as inputs to a program simulating the horizon attitude computer to obtain:

1. Attitude errors relative to the actual earth; and
2. Attitude errors relative to the ideal earth.

The satellite control system responds to the former when it should be adjusting to the latter. Any difference between the attitude errors computed for (1) and (2) is due to the anomalous effect of clouds. With these two sets of attitude data it is a simple matter to determine the degree to which the actual satellite attitude departs from the attitude indicated by telemetry.

* Data on yaw attitude is provided with variable accuracy over a portion of the daylight orbit by the course sun sensor. The greatest accuracy (about $\pm 2^\circ$) is achieved at satellite sunset. From design considerations the initial yaw error is expected to be about $\pm 1^\circ$ with a possible maximum increase of 1° at the end of six months due to gyro drift. The ± 2.0 figure appearing in the table was selected as a pessimistic estimate of maximum yaw error, taking into account the degradation in yaw control expected at the end of the satellite life.

Assume 2° Yaw Error

In this case the error due to input signal has been removed from pitch and roll by the aforementioned technique. The $\pm 2.0^\circ$ error in yaw is retained. The total error in pitch and roll is now the sum of items 2, 4 and 5 in Table 1a.

Measure Yaw Error

This is the limiting case where pitch and roll errors are reduced as in the previous paragraph; and, in addition, it is assumed that yaw error is measured with the same order of accuracy as the other two axial components. The maximum error for all three axes is now the sum of items 2, 4 and 5 in Table 1a. This degree of accuracy could be achieved for the daylight orbit with a fine sun sensor of optimum design.

THE EFFECT OF ATTITUDE ERRORS ON THE ACCURACY OF GEOGRAPHIC REFERENCING

To be useful for either operational or research purposes the picture data from meteorological satellites must be provided with geographic referencing in the form of latitude-longitude grids. It is clear that uncorrected errors in satellite attitude will be reflected in location errors for picture elements relative to the surface of the earth. By means of spherical trigonometry it is possible to map angles measured at the satellite (i.e. attitude errors) into corresponding arcs on the surface of the earth representing the displacement of picture elements. Equations for this transformation are derived in Appendix B. These equations have been used to calculate gridding errors corresponding to the attitude errors associated with each of the techniques listed in Table 1b. Results are summarized in Table 2. Complete tabulations and graphs are presented in Appendix B.

In Table 2 the heading "angle from PP" (principal point), referring to gridding errors, denotes an angle subtended at the satellite by an earth arc extending from the center picture principle point along the major axis (i. e., a perpendicular to the subsatellite point track bisecting the edges of the two side pictures) of the three picture area. The field of view of each camera is 37° with a 2° overlap, giving a total field of view of 53.5° on each side of the center camera principal point. In Table 2 gridding errors are shown for the center picture principal point, center picture edge, side picture center and side picture edge.

The mean maximum gridding error (see Appendix B, page 17) over the three picture area appears on the bottom line.

Note that gridding errors with the present design, disregarding telemetry, are about three times as large as those associated with the original design. When telemetry is used with the present design the errors are reduced to twice the original values. With the scanner pulse reconstruction technique the original design errors would be reduced by about 20 percent if a 2° yaw were experienced and by about 50 percent if yaw could be measured accurately.

It should be noted that the accuracy of the present control system would equal or exceed the original design specifications if the effect of input signal error could be removed.

Table 2
Nimbus Attitude and Gridding Errors for an orbital altitude of 500 naut. mi.

Error Specifications			Original Design	Present Design		Scanner Pulse Reconstruction	
				Disregard Telemetry	Use Telemetry	Assume Yaw 2° Error	Measure Yaw Error
Attitude Errors (degrees)	Pitch		±1	±1.5	±1.1	±0.5	±0.5
	Roll		±1	±3	±2.3	±0.5	±0.5
	Yaw		±1	±2	±2	±2	±0.7
Gridding Errors (naut. mi.)	Angle from PP	Location in Picture					
	0°	Principal Point, Center Picture	9	31	21	5	5
	18.5°	Edge, Center Picture	11	38	27	8	7
	35°	Center, Side Picture	20	56	45	18	13
	53.5°	Edge, Side Picture	56	169	123	42	28
Mean Maximum Gridding Error (naut. mi.)			23	73	52	17	12

Gridding Errors-Nimbus A

Initially, the picture grids to be generated by the computer complex at the CDA station in Alaska will be based upon attitude data obtained from telemetry which has been smoothed to remove large errors. Thus, the mean maximum error which may be anticipated at the outset of Nimbus operations will be about 50 naut. mi. (Table 2). As experience with telemetry data increases, we may find ways of reducing this error, but the degree of improvement cannot be estimated in advance. The manipulation of telemetry data to obtain refined attitude information must be regarded as one of the experiments under the Nimbus R&D program.

Gridding Errors-Future Nimbus Satellites

Two approaches which show promise of providing more accurate attitude data in the future are the scanner pulse reconstruction method and the application of classical theoretical mechanics.

Scanner Pulse Reconstruction

Table 2 indicates that this technique offers a maximum possible reduction in gridding error of 60 percent or more compared with the "Use Telemetry" method of Nimbus A. The accuracy of this approach is contingent upon the development of a reconstruction technique with minimum sensitivity to noise in the scanner system transfer functions. So far this result has not been achieved.

If the development of this technique should prove successful, it would be necessary to make provisions on the satellite for routinely recording and transmitting the scanner data. In the Nimbus A configuration high resolution infrared radiometer (HRIR) and scanner data are fed to the same tape recorder. However, the operation of this recorder is such that it is not feasible to time-share HRIR and scanner data on a single pass. As a consequence, it is necessary to record a full orbit of either HRIR or scanner data. Data selection is made by ground command. Due to the prime importance of HRIR data, the satellite tape recorder will routinely operate in the HRIR mode. An occasional orbit of scanner data will be recorded for the purpose of checking the operation of the control system. Only in the event of failure of the HRIR system would scanner data be recorded and transmitted routinely. Accordingly, the approach adopted for Nimbus A is to analyze, on a research basis, whatever scanner data becomes available with the aim of exploring the feasibility of developing an operational technique for extracting attitude from these data. In the event that such a technique were developed, it would be necessary to modify the input equipment and input logic of the CDA computer system to accommodate the scanner data.

Theoretical Mechanics

The most powerful attack on the attitude problem entails the solution of equations governing the angular momentum vector of the satellite. As mentioned earlier, if there are no external torques acting on the vehicle, the resultant of flywheel momentum and satellite body momentum is a vector fixed in inertial space. In this case pitch, roll and yaw are defined by a third order system of differential equations which can be solved for the initial condition of zero error and zero rate in all three axes.* This set of equations represents a first approximation to the complete momentum equations, derived by omitting terms describing external torque contributions (1) at satellite separation, (2) due to pneumatic gating, and (3) caused by gravitational gradients. The solution to such a mathematical system is subject to error due to inaccurate specification of the satellite inertia tensor, uncertainties in flywheel response and pneumatic operation, as well as lack of precise knowledge about the initial motion of the vehicle.

Reduction of Yaw Error

Complete elimination of the yaw attitude error in the two present design cases (i. e. Appendix B, Table B1) would produce a *negligible* decrease in total attitude error. This is a consequence of the fact that the roll error accounts for at least 80 percent of the total error. Therefore it is not profitable to expend effort in reducing yaw error unless the input signal error affecting pitch and roll can be substantially reduced by some such technique as pulse reconstruction. (From Table B1 it is evident that yaw error becomes the prime contributor to total error once the input signal error has been eliminated).

There are two possible approaches to the problem of reducing yaw error, should this prove desirable: (1) incorporation of an improved sun sensor in the satellite control system, or (2) the development of techniques for solving the gyro equation. A sun sensor yields useful data for the

*These equations have been derived by Dr. Poritsky of the GE Advanced Technology Center (Reference 8).

daylight orbit only, hence this approach does not offer a complete solution to the problem. On the other hand the gyro equation applies to the entire orbit so that a successful technique for solving it would represent a complete solution.

Yaw Bias

The effect of yaw bias had not been taken into account in this study. The introduction of a bias would result in another source of error in our knowledge of yaw orientation, over and above the uncertainty due to inaccuracies in the course sun sensor. No attempt has been made to estimate the magnitude of errors due to this effect.

METEOROLOGICAL ASPECTS OF GRIDDING ERRORS

The degree to which errors in geographic referencing affect the usefulness of meteorological satellite data is entirely a function of the requirements which the data must fulfill. For example the field forecaster who is interested in general cloud conditions over a sizable area has far less need for exact referencing than does the researcher in tropical meteorology who is concerned with the properties and motions of cloud elements of a size near the resolution capabilities of the AVCS system.

Winds and Clouds

Relation to Winds

Satellite cloud pictures will be used in conjunction with conventional meteorological data to analyze the existing state of the atmosphere as a preparatory step to prediction. The pictures will be related to certain aspects of the wind field which provide the key to future behavior of clouds. For example, a simple prediction technique might consist of advecting the clouds with the winds at cloud level. A more sophisticated method might make use of the vorticity field as an indicator of circulation development in conjunction with the divergence field as a predictor of precipitation.

It should be noted that the location error of upper level winds relative to the observing site is about 30-50 naut. mi. due to the trajectory of balloonborne radiosondes. This error is of the same magnitude as the gridding error and obtains when the cloud picture and the wind observation are taken at the same time. Since picture taking times do not in general coincide with wind observing times it will be necessary to displace the cloud data in order to obtain coincidence. On the average this adjustment will entail the displacement of clouds by an amount corresponding to an 8 hour cloud movement. Thus the average displacement will be about 250 naut. mi. By assuming that 50 percent of this displacement could be accounted for by extrapolation or prediction, the residual uncertainty in cloud location would be about 125 naut. mi.

Cloud Life Cycle

Another important consideration in the gridding problem is the life cycle of clouds identifiable in satellite pictures. It is convenient to classify clouds in three categories, each differing from the next by approximately an order of magnitude in cloud lifetime (Table 3).

In the prediction process we are mainly concerned with cloud features which appear in pictures taken on successive passes over a particular region. Since individual cloud cells will pass through their life cycle during the interval between observation and data distribution, this category is not of interest for prediction. Cloud masses tend to have a marked diurnal variation, hence they will be only marginally identifiable at 12 hour intervals—once by AVCS, and once by HRIR—by a single Nimbus. Cloudiness in this category will be of limited use for prediction.

Cyclonic and frontal cloudiness are observable by satellites for periods of several days and hence are of immense value in the prediction process. It is this type of cloudiness which will be associated with the wind field in the preparation of cloud and precipitation forecasts. Cloud systems of this type cover areas of several tens of thousands of square miles, hence, there is obviously no need to locate individual elements of such systems with a high degree of accuracy.

Errors in Mean Cloud Properties

The life cycle of cloud elements, as well as the practical aspects of operational use, dictate that the field meteorologist concern himself with mean cloudiness over an area. We shall investigate the effect of gridding errors on his estimate of mean cloud cover. For this purpose it is convenient to consider a circle of uncertainty centered at each observed* cloud element location. The magnitude of the radius R is equal to the mean maximum gridding error (Table 2). The *actual* location of each observed cloud is assumed to be within this circle of uncertainty.

Suppose that we wish to estimate the mean cloudiness for a grid square of side S . It is obvious that the *fraction* of cloud elements *observed* within the square S which are *actually* there, is dependent upon the ratio S/R . The larger this ratio the higher the fraction of actual elements within S and vice versa. The higher the fraction the more reliable are the computations of mean properties within the square and vice versa. Thus, we may substitute errors in the computation of mean values at known locations for errors in the location of known elements. However, in the process we have registered a gain in usability since mean cloudiness expressed in 3 or 4 categories is sufficient for many purposes so that a 20 or 30 percent error in mean cloud amount is not significant.

Table 3
Cloud Life Cycle.

Type of Cloud	Order of Magnitude of Cloud Duration (hrs)
Individual cell	1
Cloud mass (e.g. cumulonimbus), squall line	10
Cyclonic and frontal cloudiness	100

*The word "observed," in this context means the location computed by a gridding method which contains errors due to uncorrected satellite attitude deviations from nominal.

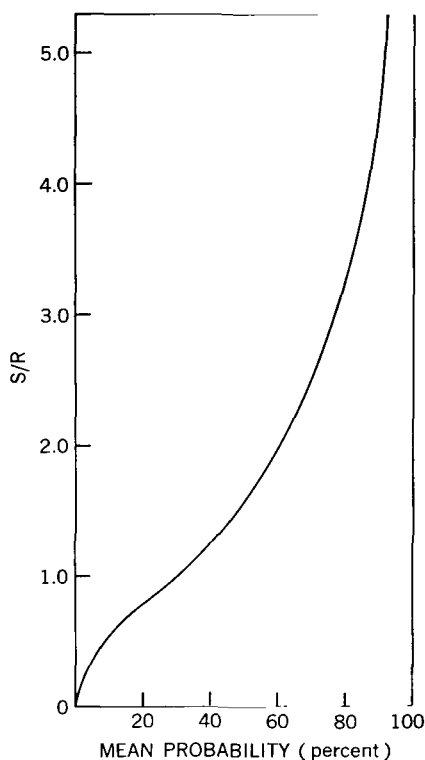


Figure 4—Mean probability of actual cloud locations in a grid square, where S is a side of a grid square, and R the radius of maximum uncertainty in cloud element location.

The mean probability that elements observed within a square S actually belong there when the radius of uncertainty is R was computed by determining the fraction of the circle R which falls within square S . This fraction was integrated along the diagonal of the square and divided by the total distance to find the desired probability. The non-dimensional parameter S/R is plotted versus probability in Figure 4.

Note that the grid square side must be at least 50 percent larger than the radius of uncertainty in order to achieve a 50 percent probability that the observed cloud elements actually belong in the square. For 75 percent probability the side must be 3 times the radius.

Applying the above criterion to the gridding errors anticipated for Nimbus A (Table 2) we find that the mean maximum error of 50 naut. mi. is compatible with 75-naut. mi. grid squares for 50 percent probability or 150 naut. mi. squares for 75 percent. In the future when the gridding error has been reduced to 20 naut. mi. the associated grid squares will shrink to 30 naut. mi. for 50 percent or 60 naut. mi. for 75 percent.

Accuracy Requirements for Cloud Location

For most operational applications of satellite picture data a maximum gridding error of about 50 naut. mi. (Reference 9) would be adequate if the confidence level were at least 70 percent that observed elements in a square actually belonged there. This criterion (Figure 4) sets the grid square side at 125 naut. mi. (about 2° of latitude). With a grid of this size the adjustment for coincidence of cloud and wind data would require an average displacement of only one grid interval.

To summarize, a 125-naut. mi. grid imposed on Nimbus A picture data will satisfy the majority of operational users.

The Weather Bureau is planning to automatically process digitized Nimbus video data to produce a rectified product on a 10-naut. mi. grid (Reference 10). If the 50 naut. mi. mean maximum gridding error were ever to occur then each of these squares would contain only 2 percent of the data which actually belongs there. If the Weather Bureau photogrammetric system (Reference 11) for attitude determination were developed the mean maximum gridding error could be reduced to about 20 naut. mi. in which case the 10-naut. mi. squares would contain 8 percent of the proper data. In order to increase the location probability to 50 percent, the square size would have to be increased to 75 naut. mi. with the 50 naut. mi. error and to 30 naut. mi. with a 20 naut. mi. error.

The above figures only apply to the case where the satellite orientation departs from nominal by the maximum conceivable amount. If the average attitude remains close to nominal then each 10 naut. mi. square will actually contain a large percentage of the cloud elements observed there.


SUMMARY AND CONCLUSIONS

More than half of the total error in both pitch and roll attitude is contributed by erroneous signal inputs to the horizon scanner system. Elimination of this error source would result in a reduction of the mean maximum gridding error from 50 naut. mi. to less than 20 naut. mi. A technique involving reconstruction of the scanner input from telemetry data shows promise for removing this error, although initial numerical solutions have exhibited instability in the presence of noise.

Since the operational user is concerned with mean cloud properties over an area rather than the location of individual elements, it is reasonable to relate gridding errors to the computation of areal means. By adopting this point of view, it is possible to show that grid squares of 2° latitude on a side are compatible with the gridding errors expected for Nimbus A.

REFERENCES

1. Barcus, R. and Spollen, F. J., "A Functional Description of the Stabilization and Control Subsystem for the Nimbus Satellite," General Electric NIMCO Systems Memo No. 1, May 1962.
2. Jensvold, R. D., "Nimbus Attitude Inputs to the Gridding Process," General Electric NIMIT PIR No. 9733-010, November 1962.
3. Spollen, F. J., "Revision A, Position Errors and Rates for NIMCO Subsystem," General Electric NIMCO PIR No. 9447-049, August 1962.
4. Hanel, R. A., Bandeen, W. R., Conrath, B. J., "The Infrared Horizon of the Planet Earth," No. X-650-62-164, Goddard Space Flight Center External Rept. August 1962.
5. Barringer, D. G., "Radius of Uncertainty due to Attitude Errors in the Nimbus Control System," General Electric NIMCO Memo No. 9752-CSA-02, January 1963.
6. Stanhouse, R. W. and Lechman, H. W., "Review of the Earth Signal for the Nimbus Attitude Sensing System," General Electric TIS Rept. No. 62SD222, November 1962.
7. Schaller, E., "Determination of Gridding Attitude using the Reconstructed Earth Emittance Waveshape," General Electric NIMIT PIR No. 9425-016, January 1963.
8. Poritsky, "Differential Equations of Roll, Pitch and Yaw Error," General Electric NIMCO Note (unnumbered), January 1963.

- 
9. Darling, E. M. Jr., "Analysis of the Contribution of Meteorological Satellite Data to the Environmental Support of Air Force Weapon Systems" (UNCL TITLE), study prepared for the Nimbus project office, August 1962 (SECRET).
 10. Bristol, C. L., "Processing Satellite Weather Data—A Status Report—Part I," Proceedings of the 1962 Fall Joint Computer Conference.
 11. Bartlett, R. B. and Greaves, J., "Nimbus Display Subsystems for Vidicon Error Removal, Attitude Determination and Meteorological Editing," ARACON Labs. Final Rept. under U. S. Weather Bureau Contract No. Cwb-10489, January 1963.

Appendix A

Scanner Pulse Reconstruction

The Nimbus scanner system, to a first approximation, may be regarded as a perfect linear system with transfer function $h(t)$, in the time domain. If the system output in response to the input function $f(t)$ is $g(t)$, then $g(t)$ may be expressed by the convolution integral

$$g(t) = \int_0^t f(\tau) h(t - \tau) d\tau = f * h.$$

The problem is as follows: Given $h(t)$, the combined optical and electronic transfer function of the scanner system, and $g(t)$ the output wave of the scanner system, find $f(t)$, the system input. For a perfect linear system the solution is straight forward.

Taking the Laplace transform of $g(t)$

$$\zeta[g(t)] = \int_0^\infty e^{-st} g(t) dt = G(s), \quad (A1)$$

$$G(s) = F(s) \times H(s), \quad (A2)$$

where G , F and H are the frequency domain equivalents of g , f and h , respectively, $F(s) = \zeta[f(t)]$, $H(s) = \zeta[h(t)]$, we have, from Equation A2,

$$F(s) = G(s) \div H(s).$$

Thus the desired function $f(t)$ is merely the inverse Laplace transform of $F(s)$:

$$f(t) = \zeta^{-1}[F(s)]$$

The uniqueness of this solution is assured by Lerch's theorem.

However the scanner system is not a perfect linear system. Mechanical, optical, and electronic noise are all present in the system transfer function. This noise is amplified by the following numerical solution which was used by Weygandt at General Electric in his first attempts to solve for $f(t)$.

The convolution was expressed as

$$g(t) = \Delta\tau \sum_{i=1}^t f\left(\frac{2i-1}{2}\right) h\left[\frac{2(t-i)+1}{2}\right].$$

By solving for $f(t)$ at successive values of t ; e. g.

$$g(1) = f\left(\frac{1}{2}\right) h\left(\frac{1}{2}\right) \Delta\tau$$

$$f\left(\frac{1}{2}\right) = \frac{g(1)}{\Delta\tau h\left(\frac{1}{2}\right)},$$

it is possible to establish the following recursion formula:

$$f\left[\frac{2t-1}{2}\right] = \frac{\frac{g(t)}{\Delta\tau} - \sum_{k=1}^{t-1} f\left[\frac{2k-1}{2}\right] g\left[\frac{2(t-k)+1}{2}\right]}{h\left(\frac{1}{2}\right)},$$

where $t \geq 2$.

The value of $g(t)$ in the numerator contains all the cumulative effects of noise from previous iterations. Furthermore, since $\Delta\tau$ is a very small time interval (about 1 millisecond) all the errors in $g(t)$ are greatly magnified. Weygandt found that this recursion formula works very well in reconstructing a simple input function (such as a step) in the absence of noise. However the formula fails when applied to complex functions.

Dr. J. G. Jewell of General Electric has investigated that scanner pulse reconstruction problem in an attempt to find solutions which are less susceptible to deterioration in the presence of noise. At present three approaches appear promising.

Appendix B

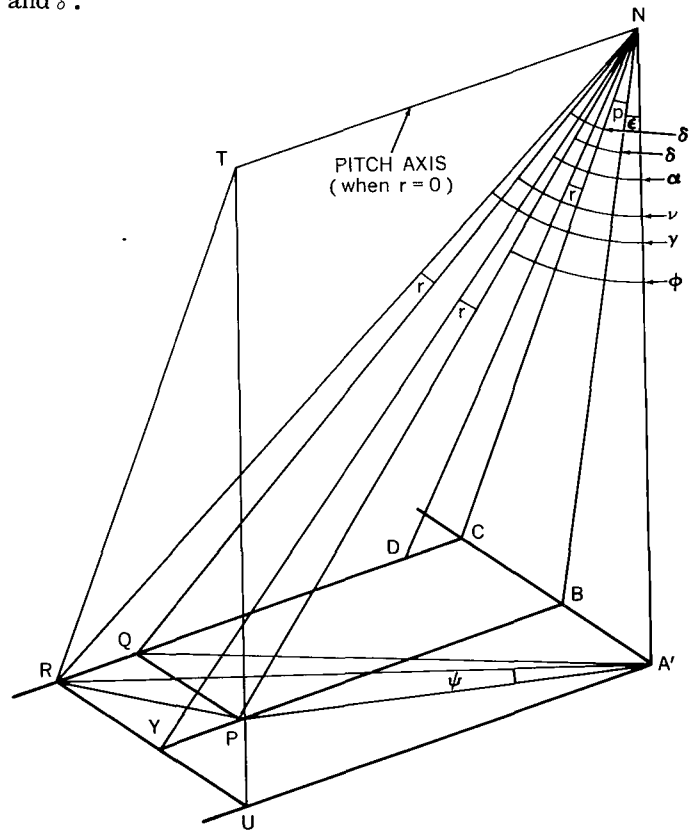
Mathematics of Gridding Errors

A separate equation has been derived for the component of gridding error contributed by each axial component of satellite attitude error. The total gridding error was obtained by combining these components as if they were independent. This procedure introduces negligible computational errors for the small angles involved (see Table 1). The gridding error geometry is shown in Figures B1, B2 and B3.

Pitch Component

The effect of the pitch error angle p is to rotate the plane YPN about TN the pitch axis so that PN rotates to QN (Figure B1). On the projection plane the pitch error is line PQ; on the earth, arc P'Q' (Figure B2). P'Q' may be found by applying the law of cosines to the spherical triangle A'P'Q'. In order to find P'Q', the great circle arcs A'P' and A'Q' must be determined as well as angle Δ , where A'P' subtends angle ϕ at the satellite, and A'Q' subtends ν . The solution involves expressing ϕ and ν in terms of the known angles p , r , ϵ and δ .

Figure B1—Projection plane geometry for pitch and roll components of gridding error. N satellite position; A', subsatellite point; $h = NA'$ satellite height; H radius of the earth. TNA'U is the plane containing the satellite pitch axis and perpendicular to the center camera focal plane. RCA'U is the plane tangent to the earth at A'. For nominal satellite attitude RCA'U is perpendicular to TNA'U as shown. A'BCN is the satellite orbital plane. A'BCN is normal to planes TNA'U, RCA'U, YPN and TNCR. In plane RCA'U the points A', B, C, D, U, P, Y, Q, R are intersections of rays emanating from the satellite and terminating at the earth's surface. Thus plane RCAU is defined as the *projection plane* for points on the earth. The following projected quantities are defined on RCAU: P, the position of a cloud element for nominal satellite attitude, is defined by angles ϵ and δ in orthogonal planes A'BCN and YPN respectively. PQ is the pitch error due to rotation of plane PNB about TN by pitch error angle p , QR is the roll error due to rotation of ray QN in plane TNCR through roll error angle r (when $p = 0$ the roll error is PY), RP is the resultant pitch-roll error.



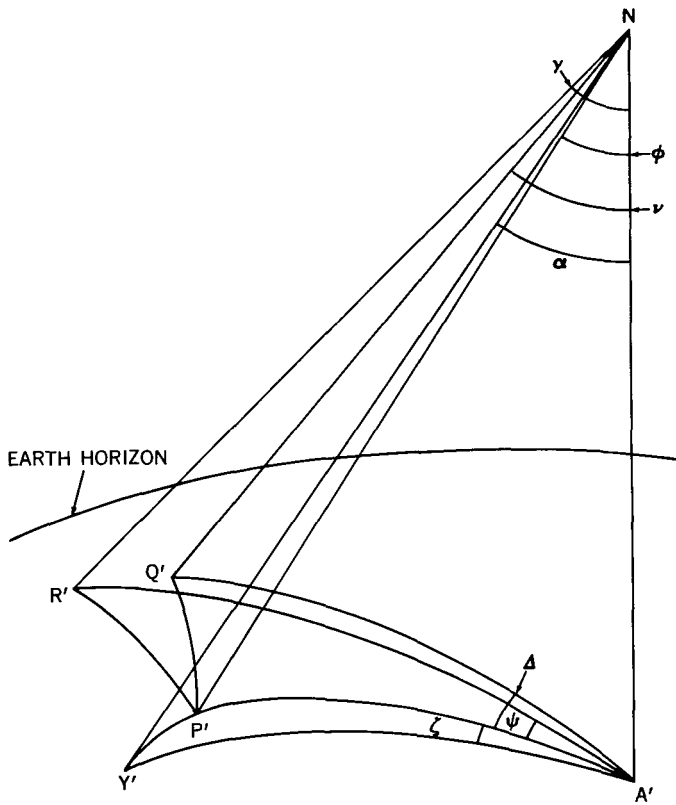


Figure B2—Spherical earth geometry for pitch and roll components of gridding error. N satellite position; A' subsatellite point; $h = NA'$ satellite height; H radius of the earth. All points designated by primed letters are earth locations of like-lettered, unprimed, projected points on plane RCA'U (Figure B1). The arcs connecting these earth points correspond to like-lettered lines in Figure B1.

We can now solve spherical triangle A'P'Q' for P'Q':

$$P'Q' = \cos^{-1}(\cos A'Q' \cos A'P' + \sin A'Q' \sin A'P' \cos \Delta), \quad (B5)$$

where, from Equation B4,

$$\begin{aligned} A'Q' &= \sin^{-1}\left(\frac{h+H}{H} \sin \nu\right) - \nu, \\ A'P' &= \sin^{-1}\left(\frac{h+H}{H} \sin \phi\right) - \phi, \end{aligned} \quad (B6)$$

and Δ is given by Equation B3.

Roll Component

The roll error, PY Figure B1, results from the rotation of PN by roll error angle τ to position YN. Proceeding as before the resultant gridding error is arc P'Y' of spherical triangle A'P'Y'

From right triangles A'CN, QCN and QNA' (Figure B1),

$$\nu = \sec^{-1}[\sec(\epsilon + p) \sec \delta]; \quad (B1)$$

from right triangles A'BN, PBN and A'BP,

$$\phi = \tan^{-1}\left[\sec \epsilon \tan \delta \sec\left[\tan^{-1}\left(\frac{\sin \epsilon}{\tan \delta}\right)\right]\right]. \quad (B2)$$

From right triangles A'CQ and A'BP:

$$\Delta = \tan^{-1}\left[\frac{\sin(\epsilon + p)}{\tan \delta}\right] - \tan^{-1}\left(\frac{\sin \epsilon}{\tan \delta}\right). \quad (B3)$$

In general the great circle arc XY (in degrees) which subtends an angle A at the satellite (measured from the local vertical) may be expressed as

$$XY = \sin^{-1}\left(\frac{h+H}{H} \sin A\right) - A, \quad (B4)$$

where h is the satellite altitude and H is the earth's radius.

(Figure B2) which we find by expressing α and ζ in terms of p, r, ϵ and δ , using right triangles in Figure B1.

From right triangles $A'BN$, YNB , and YNA' , we have

$$\alpha = \sec^{-1} [\sec \epsilon \sec (\delta + r)] \quad (B7)$$

and from $A'BP$ and $A'BY$

$$\zeta = \tan^{-1} \left(\frac{\sin \epsilon}{\tan \delta} \right) - \tan^{-1} \left[\frac{\sin \epsilon}{\tan (\delta + r)} \right] \quad (B8)$$

Solving the spherical triangle $A'P'Y'$ for $P'Y'$:

$$P'Y' = \cos^{-1} (\cos A'Y' \cos A'P' + \sin A'Y' \sin A'P' \cos \zeta) \quad (B9)$$

where, from Equation B4,

$$A'Y' = \sin^{-1} \left(\frac{h + H}{H} \sin \alpha \right) - \alpha,$$

and $A'P'$ is given by Equation B6; ζ by Equation B8.

Yaw Component

$P'V'$ (Figure B3) is the yaw error resulting from the rotation of arc $A'V'$ through yaw error angle y ($A'V' = A'P'$).

Solving the spherical triangle $P'V'A'$, we obtain

$$P'V' = \cos^{-1} (\cos^2 A'P' + \sin^2 A'P' \cos y). \quad (B10)$$

Pitch-Roll Resultant

Assuming that the satellite first pitches through angle p and then rolls through angle r , the resultant is RP in the projection plane and $R'P'$ on the earth. In this case we need angles γ, ϕ and ψ to solve spherical triangle $R'P'A'$.

In Figure B1 we have, from right triangles $A'NC$, CNR and RNA' ,

$$\gamma = \sec^{-1} [\sec (\epsilon + p) \sec (\delta + r)] \quad (B11)$$

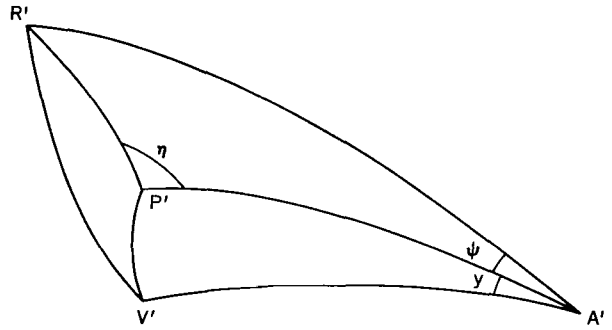


Figure B3—Spherical earth geometry of yaw error $P'V'$ and total error $R'V'$. $P'V'$ is the yaw error due to rotation of arc $A'V'$ through yaw error angle y ; $A'P' = A'V'$. $R'P'$ is the resultant pitch-roll error; and $R'V'$ is the resultant pitch-roll-yaw error.

And from right triangles A'BP and A'CR.

$$\psi = \tan^{-1} \left[\frac{\sin (\epsilon + p)}{\tan (\delta + r)} \right] - \tan^{-1} \left(\frac{\sin \epsilon}{\tan \delta} \right) . \quad (\text{B12})$$

Solving the spherical triangle R'P'A', we have

$$R'P' = \cos^{-1} (\cos A'R' \cos A'P' + \sin A'R' \sin A'P' \cos \psi) , \quad (\text{B13})$$

where, from Equation B4

$$A'R' = \sin^{-1} \left(\frac{h + H}{H} \sin \gamma \right) - \gamma ,$$

A'P' is given by Equation B6; and ψ by Equation B12.

Total Gridding Error

The total error is R'V' in Figure B3 which is the resultant of R'P' the combined pitch-roll error, and P'V' the yaw error.

Solving first for angle η , we obtain

$$\eta = \cos^{-1} \left(\frac{\cos A'R' - \cos R'P' \cos A'P'}{\sin R'P' \sin A'P'} \right) . \quad (\text{B14})$$

Finally, solving spherical triangle P'V'R':

$$R'V' = \cos^{-1} (\cos P'V' \cos R'P' - \sin P'V' \sin R'P' \sin \eta) \quad (\text{B15})$$

where P'V' is given by Equation B10, R'P' by Equation B13 and η by Equation B14. Note the sign of the second term in Equation B15 is negative if ψ is positive and vice versa.

Computation of Gridding Errors

The gridding errors calculated by the above equations are listed in Table B1 where the three axial components and the total error are tabulated versus angular distance (measured at the satellite) from the center picture principal point. The dominance of the roll error is apparent, especially at the larger angular distances, for all methods except scanner pulse reconstruction where the yaw error predominates. Pitch error makes the smallest contribution to total error in all cases.

The total gridding error has been plotted versus the angle from the center picture principal point (Figures B4-B8) for the five attitude determination methods (Table 2). In each case the

Table B1
Components of the Total Gridding Error.

Angle from Center Picture Principal Point (degrees)	Components of the Total Gridding Error (naut. mi.)			Total Gridding Error (naut. mi.)
	Pitch	Roll	Yaw	
Original Design				
0	9	9	0	9
10	9	9	2	9
20	9	10	4	11
30	10	12	7	16
40	10	18	10	25
50	11	32	13	43
53°30	13	46	17	56
Present Design (Disregard TM)				
0	13	26	0	31
10	13	28	3	34
20	14	31	7	39
30	15	39	11	49
40	18	57	16	66
50	23	108	22	116
53°30'	26	160	28	169
Present Design (Use TM)				
0	9	20	0	21
10	9	21	3	23
20	9	23	7	28
30	10	29	11	38
40	11	43	16	54
50	12	80	22	88
53°30'	14	116	28	123
Scanner Pulse Reconstruction (Yaw Error 2°)				
0	4	4	0	5
10	4	5	3	6
20	4	5	7	9
30	5	6	11	15
40	5	9	16	23
50	6	16	22	35
53°30'	7	22	28	42
Scanner Pulse Reconstruction (Measure Yaw)				
0	4	4	0	5
10	4	5	1	6
20	4	5	2	8
30	5	6	4	11
40	5	9	6	15
50	6	16	8	23
53°30'	7	22	10	28

error increases quite gradually out to about 35° (i. e. the center of the side picture) and then increases steeply from there to 53.5°, the edge of the field of view.

Mean Maximum Error

An approximation to the mean error along a diagonal from the center picture principal point to the side picture corner has been computed as follows. Equation B11 was solved for $\epsilon = 18.5^\circ$, $\delta = 53.5^\circ$, and the appropriate values of p and r for each method in Table 2 to obtain the angle γ corresponding to the diagonal in each case. The results were:

Original Design	56°49'
Present Design (Disregard telemetry)	58°46'
Present Design (Use telemetry)	58°02'
Scanner Pulse Reconstruction	56°14'

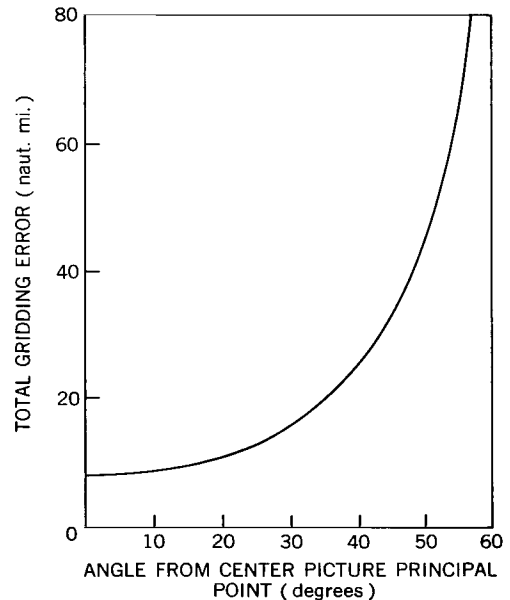


Figure B4—Gridding errors (original design). The pitch, roll and yaw errors are each ± 1 degree.

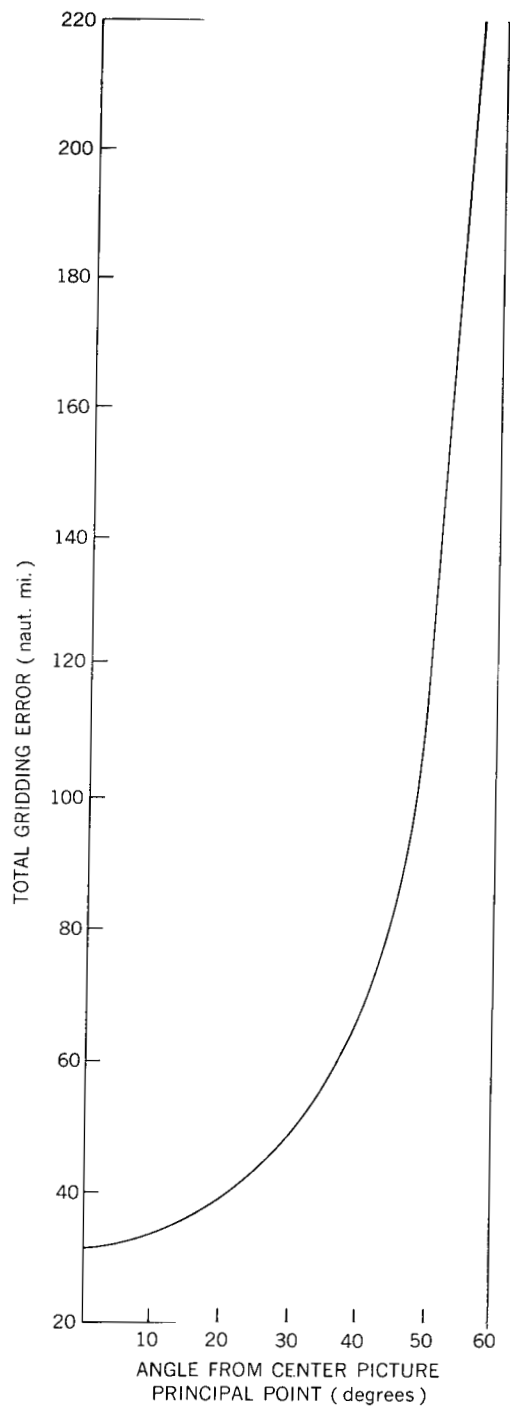


Figure B5—Gridding errors, present design (Disregard TM). The pitch error is ± 1.5 degrees; the roll error ± 3 degrees, and the yaw error ± 2 degrees.

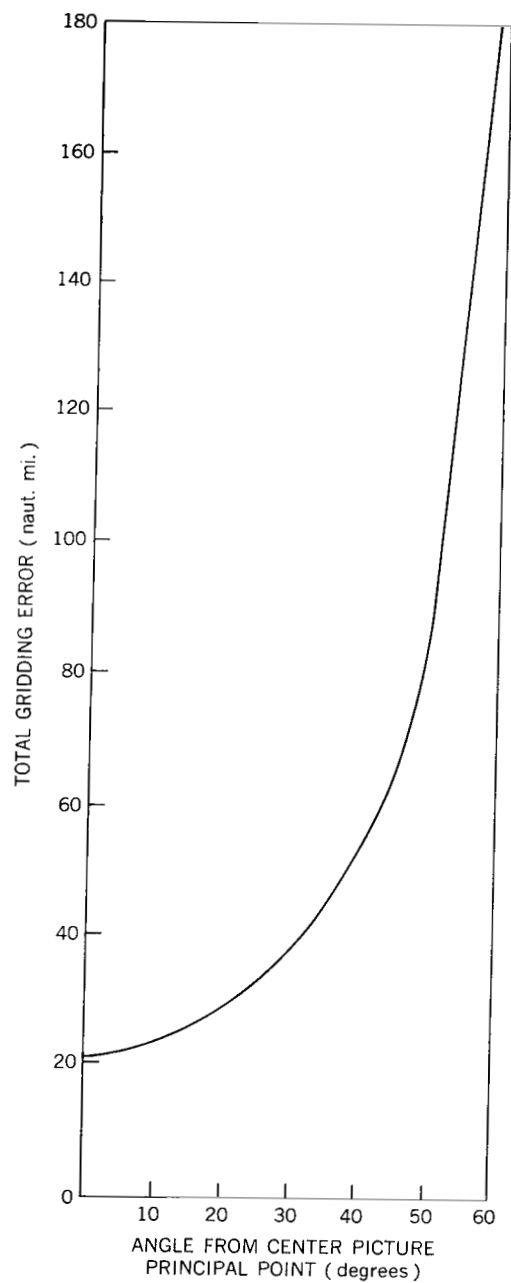


Figure B6—Gridding errors, present design (Use TM). The pitch error is ± 1.1 degrees, the roll error ± 2.3 degrees and the yaw error ± 2 degrees.

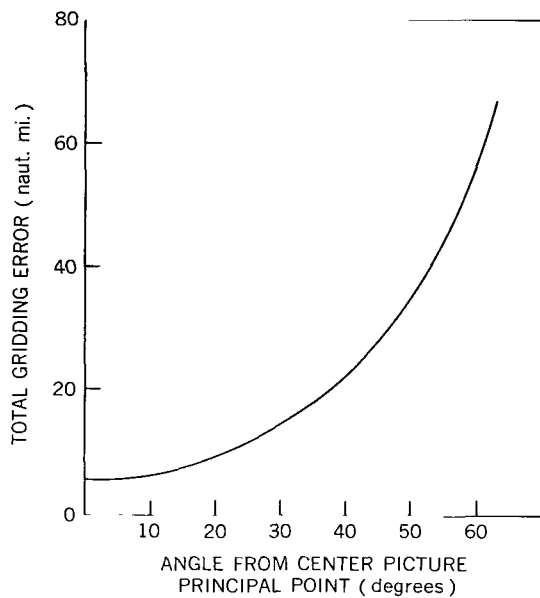


Figure B7—Gridding error, scanner pulse reconstruction technique (Disregard Yaw). The pitch error is ± 0.5 degree, the roll error ± 0.5 degree, and the yaw error ± 2 degrees.

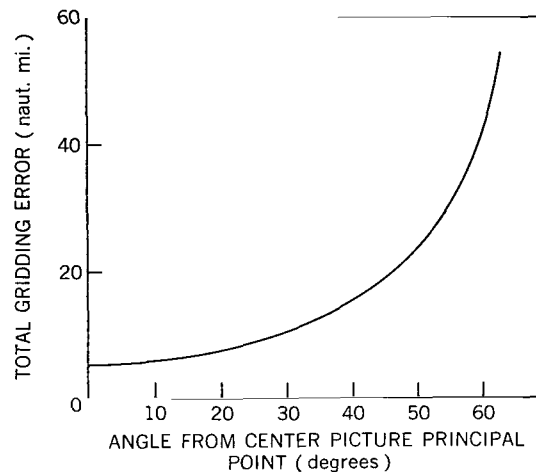


Figure B8—Gridding errors, scanner pulse reconstruction technique (Measure Yaw). The pitch error is ± 0.5 degree, the roll error ± 0.5 degree, and the yaw error ± 0.7 degree.

The mean error was computed for each case by numerically integrating the appropriate error curve (i. e. Figures B4-B8) from 0 to γ and dividing by the included area. This number has been designated as the *mean maximum error*. The value for each method is entered in the bottom row of Table 2.